SCIENTIFIC REPORTS

OPEN

SUBJECT AREAS:
METAL-ORGANIC FRAMEWORKS
POLYMER SYNTHESIS
POROUS MATERIALS
ENERGY

Received
24 June 2013

Accepted
19 August 2013

Published
10 September 2013

Correspondence and requests for materials should be addressed to G.Z. (zhugs@jlu.edu.cn)

Novel Porphyrinic Porous Organic Frameworks for High Performance Separation of Small Hydrocarbons

Heping Ma, Hao Ren, Shuang Meng, Fuxing Sun & Guangshan Zhu

State Key Laboratory of Inorganic Synthesis and Preparative Chemistry, Jilin University, Changchun, 130012, China.

A series of Porphyrinic-CTF materials are synthesized under ionothermal condition with high surface areas (>3200 m^2/g) and tunable pore sizes. The ZnP-CTFs exhibit high adsorption capacities and selectivity towards C_3H_8, and C_2H_6 over CH_4 as IAST prediction. Furthermore, we explore the utility of ZnP-CTF for gas chromatographic separation of the small hydrocarbons mixture based on their different van der waals interactions and polarizability. More importantly, the fast breakthrough test further proves that the ZnP-CTF-400 and ZnP-CTF-500 can separate the small hydrocarbons under kinetic dynamic conditions.

Small hydrocarbons (C_1, C_2 and C_3) are important energy sources and chemical feedstock in petrochemical industry. The main sources of these small hydrocarbons are natural gas and pyrolysis gas. Natural gas is actually a naturally gas mixture consisting primarily of methane, but including varying amounts of C_2H_6, C_3H_8. On the other hand, besides CH_4, the pyrolysis gas also contains $C_2 \sim C_3$ hydrocarbons and other hydrocarbons. Before transportation and utilization of these resources, they must undergo processing for upgrading and purification from their raw gases mixtures. Ordinarily, a simple temperature swing distillation can recover most of heavier hydrocarbons[1,2]. The small hydrocarbons with low boiling points are generally purified via cryogenic distillation to obtain high-grade single-component gas product, which requires high energy consumption[3]. The pressure swing adsorption (PSA) process is a cost-effective and highly efficient technique for separating small hydrocarbons from their mixture[4–6]. In the PSA process, the separation efficiency basically depend on solid adsorbents with specific adsorption properties. Thus, extensive efforts have been made to develop efficient solid adsorbents for PSA technology[7–10].

Typically, PSA is carried out under kinetic dynamic conditions and run a cycle in several minutes. To meet this challenge, the adsorbent must possess a fast separation ability. Chemisorption based adsorbents are not really suitable for this process. Porous solid materials, such as zeolites, activated carbons have been proved highly impressive adsorbents for physical adsorption and separation. However, even these traditional adsorbents exhibit a low separation capacity and selectivity in the process of separating small hydrocarbons mixtures. Metal organic frameworks (MOFs) or porous coordination polymers (PCPs) have been exploited as a new type of sorbents for hydrocarbon separation[11–15]. Recently, porous organic frameworks (POFs), assembled by organic building blocks via covalent bonds, have been proposed as new carriers for gas capture and storage[16–22]. Because of their controllable pore connectivity, chemical tailorability, high stability and large adsorption capacity, POFs have been emerged as appropriate candidates for the PSA processes.

Porphyrin is a kind of interesting macrocycle ligand with rich coordination chemistry in the square-planar coordination site. A large number of metal ions could be readily combined into the porphyrin center, which could serve as open metal site in POFs. Herein, we report a series of novel Zn porphyrinic-CTF materials (ZnP-CTF) with high BET surface areas and tunable pore sizes. The ZnP-CTF materials exhibit high adsorption capacities for C_2H_6 and C_3H_8 over CH_4. In addition, the selectivities of C_2H_6 and C_3H_8 towards CH_4 are evaluated by ideal adsorption solution theory (IAST). Furthermore, the excellently stable POF material exhibits high performance in Gas Chromatographic (GC) and kinetic fast breakthrough separation of small hydrocarbon mixture.

Results

Synthesis and characterization of ZnP-CTFs. The ZnP-CTF materials were synthesized by the dynamic trimerization of 5,10,15,20-Tetrakis(4-cyanophenyl)porphyrin under ionothermal conditions[23]. Under high temperature, the catalytic $ZnCl_2$ melts and then induces the polymerization of aromatic nitrile groups.

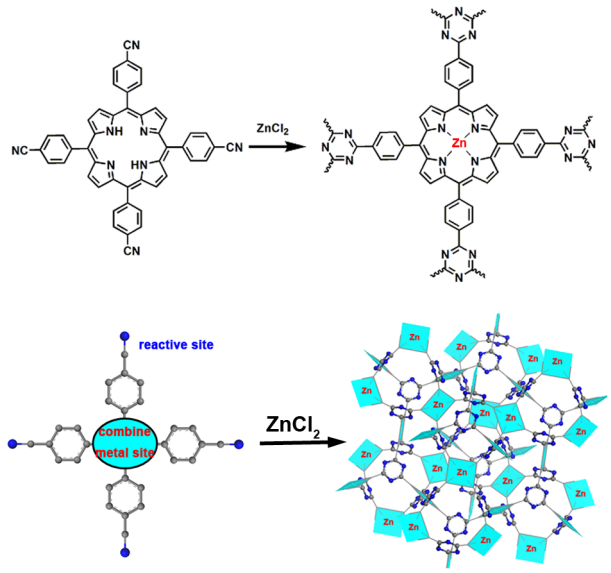

Figure 1 | **Schematic representation of the synthesis of ZnP-CTFs.**

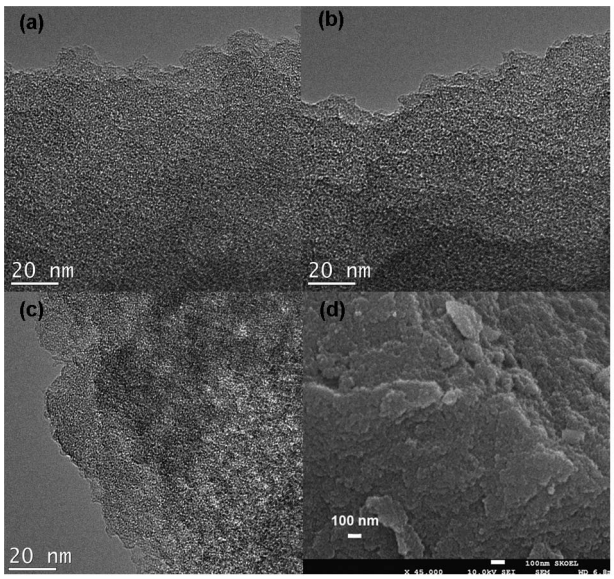

Figure 2 | **Nitrogen adsorption isotherms measured at 77 K for ZnP-CTF-400, ZnP-CTF-500 and ZnP-CTF-600.**

Meanwhile, the Zn ions could combine into the porphyrin ring center, and the Zn-porphyrin skeletons are produced (Figure 1). As documented, the character of the product was influenced by the temperature of polymerization[24,25,29]. At high temperature polymerization, the irreversible carbonization reactions ensued, coupled with the reversible trimerization of nitriles, allowing the reorganization of the dynamic triazine network to form mesopore. To tune the pore size and surface area of ZnP-CTFs, the polymerizations were carried out at 400°C, 500°C and 600°C for 40 h, respectively. The resulting products were denoted as ZnP-CTF-400, ZnP-CTF-500 and ZnP-CTF-600. The formation of polytriazine network was confirmed by FT-IR analysis (Figure S1). The disappearance of carbonitrile stretching band at 2228 cm^{-1} and the appearance of an absorption band at around 1531 cm^{-1} pointing to the characteristic of the triazine units, demonstrate the completion of the trimerization reaction. A new peak at 1005 cm^{-1} which is attributed to the absorbance of Zn–N bond in metalloporphyrin, proves the successful combination of Zn ion into the porphyrin center. For the better illustration of chemical structures of this polymer, ZnP-CTF-400 was characterized by solid-state ^{13}C and ^{15}N cross-polarization magic-angle spinning (CP/MAS) NMR. As shown in Figure S2, the NMR signal of carbon around 169.6 ppm is observed, which is assigned to carbon atom in triazine rings. The carbon signals assigned to porphyrin are also detected in the spectrum (Figure S2a). The intact structure is additionally confirmed by the ^{15}N NMR spectrum (Figure. S2b). The signal at 136.3 ppm can be ascribed to triazine moiety, the signal at 98.1 ppm is characteristic chemical shift of N atom in the porphyrin unit. Due to the decomposition of ZnP-CTFs at high temperature, we can not obtain a well-resolution carbon NMR signals for ZnP-CTF-500 and ZnP-CTF-600. Elemental analysis and Zn inductively coupled plasma (ICP) spectroscopy were performed to confirm the composition of ZnP-CTF skeletons. The weight percentages of C, H, N and Zn contents for ZnP-CTF-400 are close to the theoretical values (Table S1). Zn 2p3/2 XPS data reveal that most of the Zn ions are coordinated in porphyrin (Figure S3). When the temperature increased to 500°C and 600°C, the Zn content of ZnP-CTF materials decreased due to pyrolysis of porphyrin ring. In addition, the microstructure is studied by transmission electron microscopy (Figure 2). As can be seen, a worm-like porous texture is observed in ZnP-CTFs materials. All the ZnP-CTF materials are amorphous as confirmed by powder X-ray diffraction (PXRD) (Figure S4). Thermogravimetric analysis (TGA) of ZnP-CTF materials under air condition indicated that they have excellent thermal stability above 400°C (Figure S5).

The porosity and pore structures of ZnP-CTFs were investigated by nitrogen sorption measurement at 77 K. As shown in Figure 3, ZnP-CTF-400 exhibits Type-I isotherm, which is the typical feature of microporous materials. When temperature increases to 600°C, the isotherms of ZnP-CTF-600 displays type IV isotherm, indicating the formation of mesopores. The existence of mesopore can also be demonstrated by the plots of the NL-DFT pore size distributions of ZnP-CTF-600 (Figure S6). For clear illustration, a series of pore parameters derived from the nitrogen isotherms are listed in Table 1, including Brunauer-Emmett-Teller (BET) and Langmuir surface areas, pore sizes, total pore volumes and micropore volumes. The Langmuir surface area of ZnP-CTF-500 reaches 3218 m^2/g, which is higher than some other porphyrin-based porous organic frameworks (Table S2)[26–29].

Gas adsorption. Given ZnP-CTF materials have large surface area, abundant nitrogen atoms and micro- and mesoporous bi-modal pore system in the frameworks, we examined their CH_4, C_2H_6 and

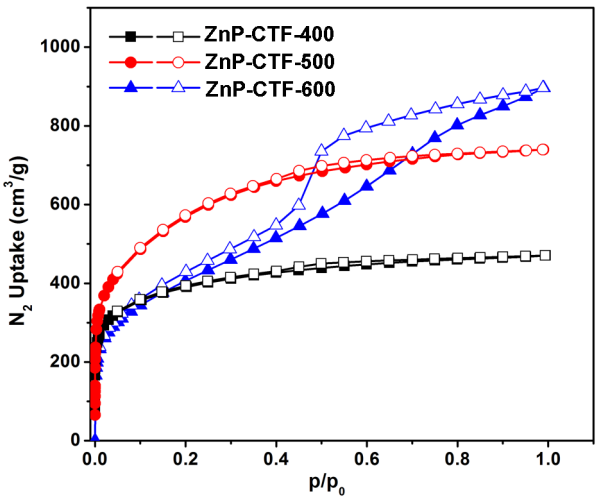

Figure 3 | **TEM images of ZnP-CTF-400 (a), ZnP-CTF-500 (b) and ZnP-CTF-600 (c); SEM image of ZnP-CTF-400 (d).**

Table 1 | Porous characteristics of ZnP-CTFs materials prepared using different temperature

Material	$S_{langmuir}$ [m^2/g]	S_{BET} [m^2/g]	Total Pore Volume (cm^3/g)	Microporous Volume (cm^3/g)	Average Pore size (nm)
ZnP-CTF-400	1766	1411	0.68	0.56	1.0
ZnP-CTF-500	3218	1848	1.1	0.61	1.3
ZnP-CTF-600	2700	1331	1.34	0.28	5

C_3H_8 adsorption isotherms at 273 K and 298 K, respectively. As shown in Figure 4a–4c and Figure S8, all gas adsorption isotherms are reversible, indicating the materials can be easily regenerated. At 298 K and 101 kPa, the C_3H_8 uptake for ZnP-CTF-400, ZnP-CTF-500 and ZnP-CTF-600 is 112 cm^3/g, 161 cm^3/g and 103 cm^3/g, respectively. The C_2H_6 uptake is 70 cm^3/g for ZnP-CTF-400, 90 cm^3/g for ZnP-CTF-500 and 54 cm^3/g for ZnP-CTF-600 under the same conditions. It is found that the ZnP-CTF materials show low adsorption capacity for CH_4 under this condition. The CH_4 uptake is 11 cm^3/g for ZnP-CTF-400, 15 cm^3/g for ZnP-CTF-500 and 9 cm^3/g for ZnP-CTF-600, respectively. Because ZnP-CTFs possess larger surface areas, they could take more C_2 and C_3 hydrocarbons than NaX zeolite and some previously reported MOFs but smaller than MOF-74 materials[11–15]. Importantly, the uptake amounts at P = 101 kPa vary so much indicating that there is an odds for the purification of the small hydrocarbon mixtures according to the number of carbon atoms.

Based on the adsorption isotherms at 273 K and 298 K, the isosteric heats of adsorption (Q_{st}) of ZnP-CTFs are calculated to estimate their affinity with probe molecules. As shown in Figure 4d–4f, a

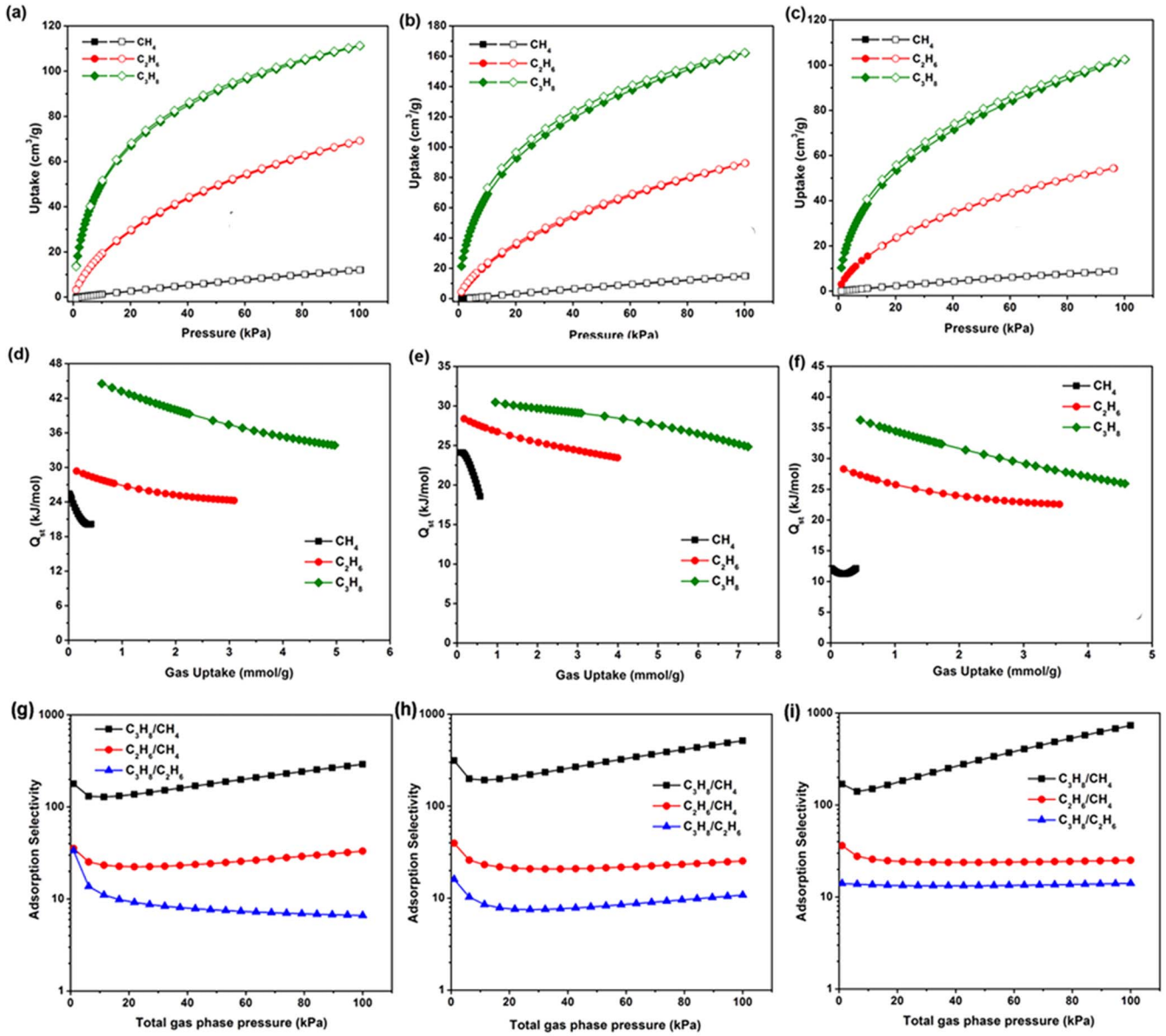

Figure 4 | Gas uptake isotherms for (a) ZnP-CTF-400, (b) ZnP-CTF-500 and (c) ZnP-CTF-600 at 298 K, 101 kPa (black CH_4, red C_2H_6, and olive C_3H_8); The isosteric heats of adsorption for ZnP-CTF-400 (d) ZnP-CTF-500 (e) and ZnP-CTF-600 (f) in function of the gas uptake (black for CH_4, red for C_2H_6 and olive C_3H_8). IAST predicted equimolar gas mixture adsorption selectivities for (g) ZnP-CTF-400, (h) ZnP-CTF-500 and (i) ZnP-CTF-600 (black square for C_3H_8/CH_4, red circle for C_2H_6/CH_4 and blue triangle C_3H_8/C_2H_6) at 298K, 101 kPa.

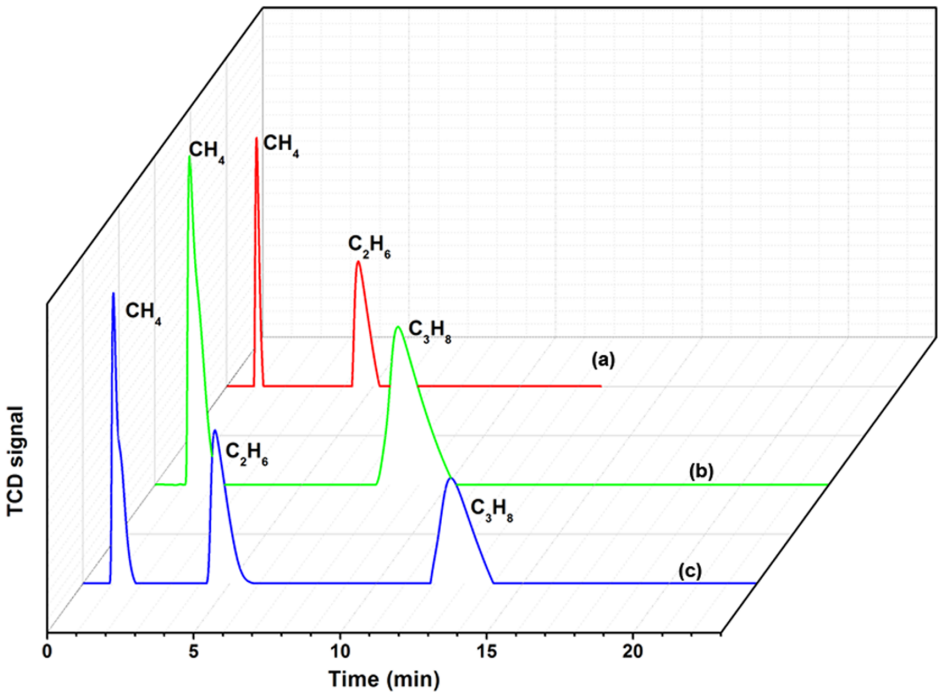

Figure 5 | Chromatograms of gas mixtures separated on a ZnP-CTF-400 column: (a) separation of C_2H_6/CH_4, (b) separation of C_3H_8/CH_4 and (c) separation of C_3H_8, C_2H_6 and CH_4 mixtures.

notably high Q_{st} values for ZnP-CTF-400 (C_3H_8: 38–45 kJ/mol; C_2H_6: 25–30 kJ/mol and CH_4: 19–25 kJ/mol) are obtained. The strong interaction between ZnP-CTF-400 and gas molecules could be attributed to uniform micropores in the framework. Comparing with ZnP-CTF-500 and ZnP-CTF-600, the smaller pore size of ZnP-CTF-400 would lead to an overlap of the van der waals forces of neighboring gas molecules, thus giving rise to more stronger interaction.

Ideal adsorbed solution theory simulation. The adsorption selectivities of ZnP-CTF materials for C_2H_6 and C_3H_8 over CH_4 in an equimolar gas mixture are evaluated by ideal adsorption solution theory (IAST). As shown in Figure 4g–4i, the selectivities of C_3H_8 towards CH_4 are in 290 for ZnP-CTF-400, 513 for ZnP-CTF-500 and 733 for ZnP-CTF-600, at 298 K and 101 kPa, respectively. The high selectivities of ZnP-CTFs make the separation of C_3H_8 from natural gas highly feasible. The C_2H_6/CH_4 selectivity of ZnP-CTF-400, ZnP-CTF-500 and ZnP-CTF-600 are 33, 26 and 25 under the same conditions (Table S3). We also investigate the C_3H_8/C_2H_6 separation ability at 298 K of ZnP-CTF materials. ZnP-CTF-600, which has more mesopores, exhibits a higher C_3H_8/C_2H_6 selectivity (15) than ZnP-CTF-500 (11) and ZnP-CTF-400 (9) under 101 kPa and 298 K.

Gas chromatographic separation. Encouraged by the adsorption interactions of ZnP-CTF materials for C_3H_8, C_2H_6 and CH_4, together with their high selectivities, we also explored the ability of ZnP-CTF-400 for kinetic separation of the small hydrocarbon molecules in Gas Chromatographic. The GC separation of $C_1 \sim C_3$ are performed by a chromatographic column (180 × 2 mm) packed with 190 mg ZnP-CTF-400. As shown in Figure 5, the ZnP-CTF-400 column can clearly separate small hydrocarbons mixture due to their different carbon atoms. Both C_2H_6 and C_3H_8 achieve baseline separation from CH_4. The ZnP-CTF-400 column gives high-resolution separation of three mixtures: C_2H_6/CH_4 (Rs = 2.8), C_3H_8/CH_4 (Rs = 7.6), C_3H_8/C_2H_6 (Rs = 4.3). The high-resolution of such columns can be explained as follows: the retention of analyte on the column mainly depends on their different van der Waals interactions with the porous ZnP-CTF skeletons. The long alkane C_3H_8 has strong van der Waals interactions with porous walls than CH_4 and C_2H_6[30–33]; On other hand, the Zn ions in ZnP-CTF offer active sites to polarize gas molecule[34,35], the polarizability of C_3H_8 is larger than CH_4 and C_2H_6 (polarizability α in units of 10^{-24} cm^3: $\alpha(C_3H_8) = 6.3 > \alpha(C_2H_6) = 4.5 > \alpha(CH_4) = 2.6$). The more polarizable molecules have strong interaction with ZnP-CTF material through dispersion forces. This behavior is similar to the open metal sites effect in MOFs coated GC stationary phase[36–39].

Breakthrough experiments. Considering the potential use of ZnP-CTF material in practical separation processes, we should also evaluate it under kinetic dynamic conditions at operating temperatures and pressures. The breakthrough curve is a typical way of estimating the gas separation ability for adsorbents under flowing gas conditions, which are related to the PSA process[40]. To further evaluate the performances of ZnP-CTF materials in an actual adsorption-based separation process, we studied dynamic breakthrough separation experiments of gas mixture at ambient conditions. For a fast separation in the PSA process, the breakthrough tests of different hydrocarbon mixtures were performed using a fixed-bed column packed with ZnP-CTF-400 or ZnP-CTF-500. ZnP-CTF-400 possesses strong hydrocarbons adsorption enthalpy and ZnP-CTF-500 has large uptake capacities. The pressure in the column was maintained at 3.1 MPa which is relevant to real purification of natural gas and LNG (3–4 MPa). The breakthrough curves of ZnP-CTF-400 and ZnP-CTF-500 are shown in Figure 6. As expected from result of GC separation, in each case, CH_4 penetrated through the bed firstly, whereas the higher hydrocarbons retained in adsorbent. The results of CH_4/C_2H_6 mixture ($CH_4:C_2H_6$ = 80:20 (vol)) test in the two columns with the space velocity of 5 min^{-1} are shown in Figure 6a and 6d. After injection of the gas mixture, the appeared to be 100% pure CH_4 was detected both in ZnP-CTF-400 and ZnP-CTF-500 columns. Upon saturation of gas adsorbed in ZnP-CTF-400 column, C_2H_6 "brokethrough" around 17 min while the ZnP-CTF-500 column can retain C_2H_6 until 21 min, which means ZnP-CTF-500 have a large adsorption capacity.

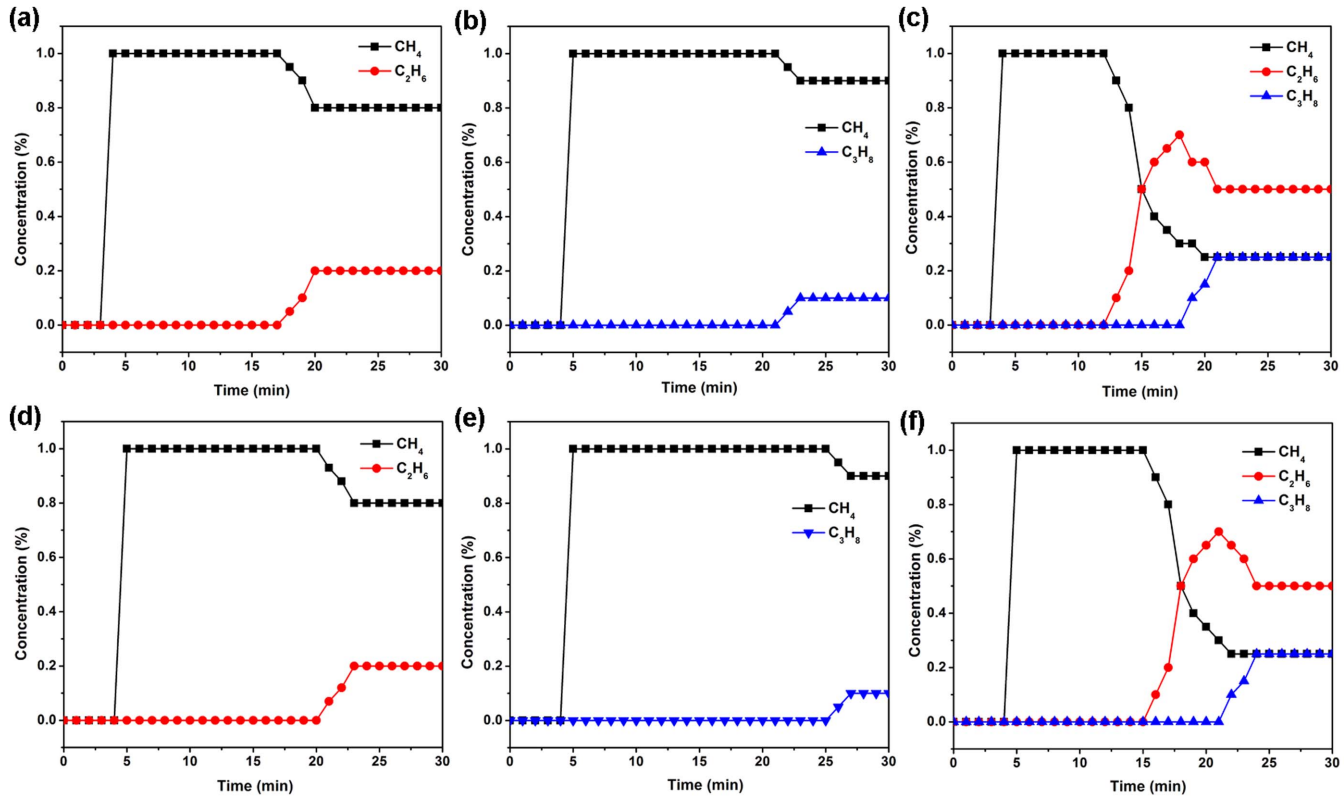

Figure 6 | Breakthrough curves of (a) C_2H_6/CH_4 mixture (20 : 80 (vol)); (b) C_3H_8/CH_4 mixture (10 : 90 (vol)); (c) $C_3H_8/C_2H_6/CH_4$ mixture (25 : 50 : 25 (vol)) for ZnP-CTF-400 and (d) C_2H_6/CH_4 mixture (20 : 80 (vol)); (e) C_3H_8/CH_4 mixture (10 : 90 (vol)); (f) $C_3H_8/C_2H_6/CH_4$ mixture (25 : 50 : 25 (vol)) for ZnP-CTF-500. These were measured at 298 K, 3 Mpa.

In the case of CH_4/C_3H_8 mixture ($CH_4 : C_3H_8 = 90 : 10$ (vol)) with space velocity of 6 min^{-1}, during 4–21 min, the ZnP-CTF-400 retained C_3H_8 and the outlet stream contained pure CH_4 (Figure 6b). After 23 min, the concentration of the outlet gas reached the feed gas composition, indicating the saturation of column. The ZnP-CTF-500 column can retain C_3H_8 for 25 min and pure CH_4 was collected during 5–25 min (Figure 6e), indicating both of packing beds can also separate CH_4 from CH_4/C_3H_8 mixture. To verify the two materials can separate of these small hydrocarbons in ternary mixed system, we measured breakthrough curves for the mixture of $CH_4/C_2H_6/C_3H_8$ (25 : 50 : 25 (vol)) with space velocity of 6 min^{-1}. As shown in Figure 6c and 6f, CH_4 with the weakest interaction with adsorbents breakthrough earliest and C_3H_8 with the strongest interaction with adsorbents retain for 18 min. Due to completely separation of CH_4 is achieved, it is possible to produce pure methane from this three-component mixture during the PSA process. The impressive performances of ZnP-CTF-400 and ZnP-CTF-500 in separation of the small hydrocarbons in the fast breakthrough test are mainly ascribed to its different interaction with guest molecules. Under the kinetic dynamic conditions, the adsorption of different gas molecules on the adsorbent is a competitive procedure. The molecules with strong affinity to adsorbent such as C_3H_8 and C_2H_6, are preferentially adsorbed on the active sites in ZnP-CTF skeleton. After adsorption of C_3H_8 and C_2H_6 molecules into the active sites, only a small amount of pore volume is left for CH_4. Thus the adsorption of CH_4 in the ZnP-CTF is suppressed and it passes through the packing column fluently. The ZnP-CTF-500 material which displays moderate heats of adsorption for C_2H_6 and C_3H_8 than ZnP-CTF-400 may have lower regeneration requirements. The significant results in physical adsorption based separations of these small hydrocarbons offer ZnP-CTF materials as a potential stepping stone to porous materials for purification of natural gas and LNG.

Discussion

In conclusion, we successfully synthesize novel ZnP-CTF materials through ionothermal reaction. By controlling synthesis temperature, the tunable surface areas and pore sizes of ZnP-CTF materials are achieved. More valuably, ZnP-CTF materials show different adsorption capacities for the small hydrocarbons according to the number of carbon atoms. The selective hydrocarbons adsorption of ZnP-CTF materials are demonstrated by IAST prediction. Furthermore, we explore the utility of ZnP-CTF-400 for high performance GC separation of small hydrocarbons mixture owing to their different van der Waals interactions and polarizability. The fast dynamic breakthrough tests further prove the ZnP-CTF-400 and ZnP-CTF-500 can separate the small hydrocarbons based on their hierarchical isosteric heats in an actual adsorption-based separation process. For the first time, we systematically investigated POFs for the hydrocarbons separation under both equilibrium and kinetic conditions. The high separation capability and selectivity offers ZnP-CTF-500 as a promising candidate for energy efficient separation of small hydrocarbons in PSA process.

Methods

Materials. All starting materials were purchased from commercial suppliers and used without further purification unless otherwise noted. Anhydrous $ZnCl_2$ was purchased from Alfa Aesar. 5,10,15,20-Tetrakis(4-cyanophenyl)porphyrin[41] was synthesized according to the previously reported method.

Synthesis of ZnP-CTFs. 5,10,15,20-Tetrakis(4-cyanophenyl)porphyrin (1 mmol) and $ZnCl_2$ (8 mmol) were transferred into a quartz ampule (3 × 12 cm) under an inert atmosphere. The ampule was evacuated, sealed, and heated to the desired temperature (400, 500, 600°C) for 40 h. The ampule was then cooled to room temperature and opened. The reaction mixture was subsequently ground and then stirred with water for 24 h. Further stirring in 0.1 M HCl for 15 h was carried out to remove the residual salt. After this purification step, the resulting black powder was filtered, washed successively with water and CH_3OH, and dried in vacuum at 150°C. ZnP-CTFs were isolated in 85–90% yield.

Ideal adsorption solution theory calculations. The ideal adsorption solution theory (IAST) was used to predict the binary mixture adsorption from the experimental pure-gas isotherms. Previous studies have shown that the IAST can predict mixture gas adsorption in many nanoporous materials, including porous-organic frameworks[42–44]. The single-component isotherms were fitted using a dual-site Langmuir-Freundlich equation (1):

$$q = q_{m1} \cdot \frac{b_1 \cdot p^{1/n_1}}{1 + b_1 \cdot p^{1/n_1}} + q_{m2} \cdot \frac{b_2 \cdot p^{1/n_2}}{1 + b_2 \cdot p^{1/n_2}} \quad (1)$$

Here, p is the pressure of the bulk gas at equilibrium with the adsorbed phase (kPa), q is the adsorbed amount per mass of adsorbent (mmol/g), q_{m1} and q_{m2} are the saturation capacities of sites 1 and 2 (mmol/g), b_1 and b_2 are the affinity coefficients of sites 1 and 2 (1/kPa), and n_1 and n_2 represent the deviations from an ideal homogeneous surface.

The IAST adsorption selectivity, S, for binary mixtures of CO_2 (1)/N_2 (2), is defined as follows equation (2):

$$S = \frac{q_1/q_2}{p_1/p_2} \quad (2)$$

where q_i and p_i (i = 1,2) are the mole fractions of component 1 and 2 in the adsorbed and bulk phases, respectively. The IAST calculations were carried out for binary mixture containing equimolar gas.

Details of the breakthrough curve measurement. Breakthrough curve measurements were performed using a home-made gas-flow system. In practice, the experiment is conducted as follows: The adsorbent ZnP-CTF-400 was filled into the column with a length of 150 mm and an internal diameter of 5 mm. before test, the column was activated in flow of Ar for 24 h. The pressure in the column was maintained at 3.1 MPa. The experiments were performed at 298 K. For the CH_4/C_2H_6 mixture gas, the gas fraction was $CH_4 : C_2H_6 = 80 : 20$ (v/v) with a space velocity of 5 min^{-1}. For the CH_4/C_3H_8, the gas component was $CH_4 : C_3H_8 = 90 : 10$ (v/v) with a space velocity of 6 min^{-1}. For the $CH_4/C_2H_6/C_3H_8$ mixture gas, the gas component was $CH_4 : C_2H_6 : C_3H_8 = 25 : 50 : 25$ (v/v/v) with a space velocity of 6 min^{-1}. The flow rates of all of the pure gases were regulated by mass flow controllers (0–100 mL min^{-1}). The gas mixture was first sent to the gas chromatograph through bypass line and measured its component before the breakthrough measurements. The relative amounts of the effluent gases passing through the column were monitored by GC.

1. Ding, Z. Y. & Lattner, J. R. Recovery of C4 olefins from a product stream comprising C_4 olefins, dimethyl ether and C_{5+} hydrocarbons. *U.S. Pat.* US 2006/7060865 (2006).
2. Howard, L. J. & Rowles, H. C. Low pressure process for C_{3+} liquids recovery from process product gas. *U.S. Pat.* US 1988/4734115 (1988).
3. Rojey, A. & Jaffret, C. *NATURAL GAS: PRODUCTION, PROCESSING, TRANSPORT*. Editions Technip, Paris, (1997).
4. Magnowski, N. B. K., Avila, A. M., Lin, C. C. H., Shi, M. & Kuznicki, S. M. Extraction of ethane from natural gas by adsorption on modified ETS-10. *Chem. Eng. Sci.* **66**, 1697–1701 (2011).
5. Arruebo, M., Coronas, J., Menendez, M. & Santamaria, J. Separation of hydrocarbons from natural gas using silicalite membranes. *Sep. Purif. Tech.* **25**, 275–286 (2001).
6. Triebe, R., Tezel, W. F. H. & Khulbe, K. C. Adsorption of methane, ethane and ethylene on molecular sieve zeolites. *Gas Sep. Purif.* **10**, 81–84 (1996).
7. Peralta, D. G. *et al.* Comparison of the Behavior of Metal–Organic Frameworks and Zeolites for Hydrocarbon Separations. *J. Am. Chem. Soc.* **134**, 8115–8126 (2012).
8. Reyes, S. *et al.* Separation of methane from higher carbon number hydrocarbons utilizing zeolitic imidazolate framework materials. *US Pat.* US 2009/0216059 A1 (2009).
9. Kuznicki, S. M., Avila, A. M., Shi, M. & Strom, V. L. Removal of ethane from natural gas at high pressure. *US Pat.* US 2011/0315012 A1 (2011).
10. Yang, R. T. *GAS SEPARATION BY ADSORPTION PROCESSES*. Imperial College Press, (1997).
11. He, Y. Z. *et al.* High Separation Capacity and Selectivity of C_2 Hydrocarbons over Methane within a Microporous Metal–Organic Framework at Room Temperature. *Chem. Eur. J.* **18**, 1901–1904 (2012).
12. He, Y. *et al.* A robust doubly interpenetrated metal–organic framework constructed from a novel aromatic tricarboxylate for highly selective separation of small hydrocarbons. *Chem. Commun.* **48**, 6493–6495 (2012).
13. He, Y., Krishna, R. & Chen, B. Metal–organic frameworks with potential for energy-efficient adsorptive separation of light hydrocarbons. *Energy Environ. Sci.* **5**, 9107–9120 (2012).
14. Horike, S., Inubushi, Y., Hori, T., Fukushima, T. & Kitagawa, S. A solid solution approach to 2D coordination polymers for CH_4/CO_2 and CH_4/C_2H_6 gas separation: equilibrium and kinetic studies. *Chem. Sci.* **3**, 116–120 (2012).
15. Duan, J. *et al.* High CO_2/CH_4 and C_2 Hydrocarbons/CH_4 Selectivity in a Chemically Robust Porous Coordination Polymer. *Adv. Funct. Mater.* DOI: 10.1002/adfm.201203288 (2013).
16. McKeown, N. B. & Budd, P. M. Polymers of intrinsic microporosity (PIMs): organic materials for membrane separations, heterogeneous catalysis and hydrogen storage. *Chem. Soc. Rev.* **35**, 675–683 (2006).
17. Dawson, R., Cooper, A. I. & Adams, D. J. Nanoporous organic polymer networks. *Prog. Polym. Sci.* **37**, 530–563 (2012).
18. Wu, D., Xu, F., Sun, B., Fu, R., He, H. & Matyjaszewski, K. Design and Preparation of Porous Polymers. *Chem. Rev.* **112**, 3959–4015 (2012).
19. Ben, T. *et al.* Targeted Synthesis of a Porous Aromatic Framework with High Stability and Exceptionally High Surface Area. *Angew. Chem. Int. Ed.* **48**, 9457–9460 (2009).
20. Ma, H. *et al.* Novel lithium-loaded porous aromatic framework for efficient CO_2 and H_2 uptake. *J. Mater. Chem. A* **1**, 752–758 (2013).
21. Lu, W. *et al.* Porous Polymer Networks: Synthesis, Porosity, and Applications in Gas Storage/Separation. *Chem. Mater.* **22**, 5964–5972 (2010).
22. Luo, Y., Li, B., Wang, W., Wu, K. & Tan, B. Hypercrosslinked Aromatic Heterocyclic Microporous Polymers: A New Class of Highly Selective CO_2 Capturing Materials. *Adv. Mater.* **24**, 5703–5707 (2012).
23. Kuhn, P., Antonietti, M. & Thomas, A. Porous, Covalent Triazine-Based Frameworks Prepared by Ionothermal Synthesis. *Angew. Chem. Int. Ed.* **47**, 3450–3453 (2008).
24. Kuhn, P., Forget, A., Su, D., Thomas, A. & Antonietti, M. From Microporous Regular Frameworks to Mesoporous Materials with Ultrahigh Surface Area: Dynamic Reorganization of Porous Polymer Networks. *J. Am. Chem. Soc.* **130**, 13333–13337 (2008).
25. Kuhn, P., Thomas, A. & Antonietti, M. Toward Tailorable Porous Organic Polymer Networks: A High-Temperature Dynamic Polymerization Scheme Based on Aromatic Nitriles. *Macromolecules* **42**, 319–326 (2009).
26. Wang, X. S. *et al.* A porous covalent porphyrin framework with exceptional uptake capacity of saturated hydrocarbons for oil spill cleanup. *Chem. Commun.* **49**, 1533–1535 (2013).
27. Liu, X., Xu, Y., Guo, Z., Nagai, A. & Jiang, D. Super absorbent conjugated microporous polymers: a synergistic structural effect on the exceptional uptake of amines. *Chem. Commun.* **49**, 3233–3235 (2013).
28. Wang, Z. *et al.* Nanoporous Porphyrin Polymers for Gas Storage and Separation. *Macromolecules* **45**, 7413–7419 (2012).
29. Liu, X. *et al.* Enhanced carbon dioxide uptake by metalloporphyrin-based microporous covalent triazine framework. *Poly. Chem.* **4**, 2445–2448 (2013).
30. Chen, B. L. *et al.* A Microporous Metal–Organic Framework for Gas-Chromatographic Separation of Alkanes. *Angew. Chem., Int. Ed.* **45**, 1390–1393 (2006).
31. Chang, N., Gu, Z. Y. & Yan, X. P. Zeolitic Imidazolate Framework-8 Nanocrystal Coated Capillary for Molecular Sieving of Branched Alkanes from Linear Alkanes along with High-Resolution Chromatographic Separation of Linear Alkanes. *J. Am. Chem. Soc.* **132**, 13645–13647 (2010).
32. Gu, Z. Y., Jiang, J. Q. & Yan, X. P. Fabrication of isoreticular metal-organic framework coated capillary columns for high-resolution gas chromatographic separation of persistent organic pollutants. *Anal. Chem.* **83**, 5093–5100 (2011).
33. Zhao, H. *et al.* Target synthesis of a novel porous aromatic framework and its highly selective separation of CO_2/CH_4. *Chem. Commun.* **49**, 2780–2782 (2013).
34. Kazansky, V. B., Subbotina, I. R., Rane, N., Santen, R. A. & Hensen, E. J. M. On two alternative mechanisms of ethane activation over ZSM-5 zeolite modified by Zn^{2+} and Ga^{1+} cations. *Phys. Chem. Chem. Phys.* **7**, 3088–3092 (2005).
35. Kazansky, V. B. & Pidko, E. A. Intensities of IR Stretching Bands as a Criterion of Polarization and Initial Chemical Activation of Adsorbed Molecules in Acid Catalysis. Ethane Adsorption and Dehydrogenation by Zinc Ions in ZnZSM-5 Zeolite. *J. Phys. Chem. B* **109**, 2103–2108 (2005).
36. Münch, A. S. & Mertens, F. O. R. L. HKUST-1 as an open metal site gas chromatographic stationary phase—capillary preparation, separation of small hydrocarbons and electron donating compounds, determination of thermodynamic data. *J. Mater. Chem.* **22**, 10228–10234 (2012).
37. Ahmed, A. *et al.* Silica SOS@HKUST-1 composite microspheres as easily packed stationary phases for fast separation. *J. Mater. Chem. A* **1**, 3276–3286 (2013).
38. Fu, Y. Y., Yang, C. X. & Yan, X. P. Control of the coordination status of the open metal sites in metal-organic frameworks for high performance separation of polar compounds. *Langmuir* **28**, 6794–6802 (2012).
39. Borjigin, T., Sun, F., Zhang, J., Cai, K., Ren, H. & Zhu, G. A microporous metal-organic framework with high stability for GC separation of alcohols from water. *Chem. Commun.* **48**, 7613–7615 (2012).
40. Doong, S. J. & Yang, R. T. Bulk separation of multicomponent gas mixtures by pressure swing adsorption: pore/surface diffusion and equilibrium models. *AIChE J.* **32**, 397–409 (1986).
41. Gauuan, P. J. F. M. *et al.* Superoxide dismutase mimetics: synthesis and structure–activity relationship study of MnTBAP analogues. *Bioorg. Med. Chem.* **10**, 3013–3021 (2002).
42. Myers, A. L. & Prausnitz, J. M. Thermodynamics of mixed-gas adsorption. *AIChE J.* **11**, 121–127 (1965).
43. Bae, Y., Mulfort, K. L., Frost, H., Ryan, P., Punnathanam, S., Broadbelt, L. J., Hupp, J. T. & Snurr, R. Q. Separation of CO_2 from CH_4 Using Mixed-Ligand Metal-Organic Frameworks. *Langmuir*, **24**, 8592–8598 (2008).

44. Reich, T. E., Behera, S., Jackson, K. T., Jena, P. & El-Kaderi, H. M. Highly selective CO_2/CH_4 gas uptake by a halogen-decorated borazine-linked polymer. *J. Mater. Chem.* **22**, 13524–13528 (2012).

Acknowledgments

We are grateful to the financial support from National Basic Research Program of China (973 Program, grant nos.2012CB821700), Major International (Regional) Joint Research Project of NSFC (grant nos. 21120102034) NSFC (grant nos. 20831002) and Australian Research Council Future Fellowship (FT100101059).

Author contributions

H.M. designed and performed most of experiments. S.M., G.Z. and F.S. analyzed date. H.R. and H.M. co-wrote the paper. All authors contributed to results analysis and discussion. All authors reviewed the manuscript.

Additional information

Supplementary information accompanies this paper at http://www.nature.com/scientificreports

Competing financial interests: The authors declare no competing financial interests.

How to cite this article: Ma, H., Ren, H., Meng, S., Sun, F. & Zhu, G. Novel Porphyrinic Porous Organic Frameworks for High Performance Separation of Small Hydrocarbons. *Sci. Rep.* **3**, 2611; DOI:10.1038/srep02611 (2013).